Smart Structures and Systems, *Vol. 35, No. 2 (2025) 65-75*
https://doi.org/10.12989/sss.2025.35.2.065

Long short-term memory with wavelet decomposition for wind speed predicting based on SHM data

Yang Ding [1,2], Ning-Yi Liang [3,4], Xue-Song Zhang [1], Jun Wang [2] and Chao-Qun Zeng*[5]

[1] *State Key Laboratory of Mountain Bridge and Tunnel Engineering, Chongqing Jiaotong University, Chongqing 400074, China*
[2] *Department of Civil Engineering, Hangzhou City University, Hangzhou 310015, China*
[3] *School of Civil Engineering, Changsha University of Science & Technology, Changsha 410114, China*
[4] *Zhejiang Science Research Institute of Transportation, Hangzhou 310023, China*
[5] *School of Automobile and Transportation, Shenzhen Polytechnic University, Shenzhen, Guangdong 518055, China*

(*Received May 9, 2024, Revised November 29, 2024, Accepted January 14, 2025*)

Abstract. The wind field environment surrounding long-span bridges is characterized by its complexity and variability, resulting in wind speed exhibiting random, nonlinear, and uncertain behavior. To enhance bridge safety and mitigate the impact of wind speed, it is crucial to establish a reliable wind speed prediction model. In this study, a structural health monitoring (SHM) system was deployed on a long-span bridge to collect extensive wind speed data, which was subsequently denoised using the wavelet decomposition (WD) method. Leveraging the long short-term memory (LSTM) approach, a wind speed prediction model (WD-LSTM) was developed. The study focuses on investigating the effects of three different thresholds (Bayesian threshold, SURE threshold, and Minmax threshold) in the WD method, the number of hidden units (2, 4, 8, 16, 32, 64, 128, 256, and 512) in the WD-LSTM model, and the number of inputs (one-step prediction, five-step prediction, ten-step prediction, and twenty-step prediction) in the WD-LSTM model on the prediction performance of wind speed. Evaluation metrics such as RMSE and R^2 are employed for this analysis. Furthermore, the calculation time of the WD-LSTM prediction models with different hidden units and inputs is compared. Finally, an optimal WD-LSTM prediction model is proposed, taking into account both prediction accuracy and calculation time.

Keywords: long-span bridge; long short-term memory; structural health monitoring; wavelet decomposition; wind speed prediction

1. Introduction

Wind is a common and hazardous weather condition that poses a significant risk to traffic safety (Park *et al*. 2023, Ding *et al*. 2023a). The influence of wind on both vehicles and pedestrians cannot be overlooked (Sareen *et al*. 2023, Ding *et al*. 2023b). Furthermore, long-span bridges serve as critical intersections for sea-crossing highways (Ding *et al*. 2024a, Santos *et al*. 2023, Ti *et al*. 2019). The wind environment at bridge sites is characterized by variability and complexity, which further escalates the likelihood of traffic accidents (Ding *et al*. 2025, Son *et al*. 2022, Fenerci *et al*. 2017). Hence, the establishment of a reliable early warning system for strong winds is essential to mitigate the adverse impact on safe passage across the bridge.

With the continuous advancement of science and technology, an increasing number of bridges are now equipped with structural health monitoring (SHM) systems, capable of collecting extensive wind speed data (Ding *et al*. 2023c, 2024b, Li *et al*. 2006). However, these SHM systems are vulnerable to several uncertain factors, including human interference and power equipment failures, resulting in noisy monitoring data (Li *et al*. 2021). In order to tackle this issue, various data processing methods, such as wavelet decomposition (WD) (An *et al*. 2011), empirical mode decomposition (EMD) (Xu and Chen 2004), and Kalman filtering (Zhi *et al*. 2017), have been widely adopted for data denoising. Once reliable and complete monitoring data is obtained through denoising methods, in-depth analysis is necessary to enable the early warning function, such as prediction.

Currently, the field of wind speed prediction can be divided into traditional prediction methods and machine learning methods (Joseph *et al*. 2023, López and Arboleya 2022). The traditional wind speed prediction methods mainly include two types: those based on physical models and those based on statistical models (Ding *et al*. 2023d). The method based on physical models is suitable for long-term weather prediction, but its prediction accuracy may be lower for short-term wind speed prediction. Based on statistical models, such as time series analysis, regression analysis, etc., this method has simple calculations, fast prediction speed, and is suitable for short-term wind speed prediction. However, it has a strong dependence on historical data and limited predictive ability for extreme weather or emergencies (Ding *et al*. 2023e, Wang *et al*. 2024a). Machine learning methods are capable of processing large amounts of complex data and capturing the

*Corresponding author, Ph.D., Associate Professor,
E-mail: zengchaoqun@szpu.edu.cn;
ceyangding@zju.edu.cn

ISSN: 1738-1584 (Print), 1738-1991 (Online)

nonlinear changes in wind speed, especially performing well in short-term wind speed prediction. Specially, the key factors affecting the effectiveness of machine learning based wind speed prediction models mainly include data quality, model selection, parameter adjustment, and real-time data updates. In terms of model selection, it is necessary to choose a predictive model suitable for wind speed time series. In terms of data quality, it is necessary to denoise the raw data. In terms of parameter adjustment and data update, massive monitoring data is needed as a guarantee. Wang *et al*. (2018) introduced a new hybrid model for short-term wind speed prediction, focusing on a 10-minute short-term forecast period. This model combines extreme learning machines with improved complementary integrated empirical pattern decomposition with adaptive noise and autoregressive integrated moving average. Another method proposed by Liu *et al*. (2015) utilizes EMD and an improved recursive ARIMA model for short-term wind speed prediction. Experimental results demonstrated that this method outperforms traditional ARIMA models and the persistent random walk model (PRWM), providing satisfactory accuracy and time performance. Chen and Yu (2014) integrated support vector regression (SVR) with an untraced Kalman filter (UKF) based on a state-space model to enhance the accuracy of short-term wind speed sequence predictions. Results indicate that this proposed method performs better in one-step and multi-step wind speed predictions at all locations. Traditional prediction methods are based on the correlation and causality between independent and dependent variables, and do not require other correlated factors, making them simple (Liu *et al*. 2012). However, these methods often exhibit large prediction errors when the external environment undergoes significant changes (Cadenas and Rivera 2010).

In order to improve the accuracy of wind speed prediction, researchers have increasingly turned to machine learning methods (Lim *et al*. 2022, Cui *et al*. 2021). For instance, Salehi Borujeni *et al*. (2021) introduced a novel hybrid computational model based on radial basis function (RBF) artificial neural networks, which amplifies the performance of measurement correlation prediction (MCP) methods. Liu *et al*. (2021) devised a wind speed prediction model that integrates EMD with innovative recursive neural networks (RNN) and ARIMA. Concurrently, Ding *et al*. (2021) presented a short-term wind speed prediction model termed Ceemdan-SE-Improved PIO-GRNN, founded on complete ensemble empirical mode decomposition with adaptive noise (CEEMDAN), sample entropy (SE), pigeon-inspired optimization (PIO), and generalized regression neural network (GRNN). This model strives to optimize the accuracy of short-term wind speed forecasts. Furthermore, Mishra *et al*. (2020) proposed a new short-term solar forecasting model that merges deep learning (DL) technology and long-term memory networks (LSTM) with the concept of wavelet transform (WT). Lastly, Wang *et al*. (2016) devised a wind speed prediction method based on improved EMD and GA-BP neural networks.

It is evident that the predictive performance of models based on different machine learning methods can vary. Feedforward neural networks, such as BP and RBF, often struggle to predict time series data accurately as they assume no relation between the input at the current moment and the input at the next time step, unless they are enhanced (Zhang *et al*. 2021). On the other hand, RNN networks, which are cyclic neural networks with memory, excel at extracting useful information from time series data, making them highly effective for wind speed prediction. However, RNNs are prone to issues like gradient disappearance and explosion, limiting their effectiveness in processing long-term data (Wang *et al*. 2019). In contrast, LSTM is an improvement over RNN networks as it can handle long-term dependencies and effectively extract potential information from the data while preserving historical information (Wang *et al*. 2024b, Zhu *et al*. 2019). Furthermore, wind speed data is a typical time series data with temporal continuity and correlation. LSTM can effectively capture and model long-term dependencies in time series data by introducing gating mechanisms, including input gates, forget gates, and out-put gates. The unit structure of LSTM allows the network to dynamically remember and forget information when processing sequences. This ability enables LSTM to better capture the dynamic changes in wind speed data, thereby improving the accuracy of predictions.

Therefore, in order to apply wind monitoring technologies and predictive models to the maintenance and management strategies of long-span bridges to enhance their resilience and safety under fluctuating wind conditions. Firstly, the high-precision and high stability wind speed and direction sensors should be installed at key locations on the bridge to comprehensively monitor the wind environment and wind loads of the bridge project. Secondly, machine learning-based wind speed prediction model to predict the trend of wind speed changes and wind load conditions in the future, which can provide decision support for bridge maintenance and management. Finally, based on the results of the prediction model, a bridge wind-induced vibration warning system is established. All in all, this research gathered a substantial volume of wind speed data from the Structural Health Monitoring (SHM) system installed on the examined bridge. To enhance the data quality, the wind speed data underwent denoising using the Wavelet Denoising (WD) method. Subsequently, a wind speed prediction model termed WD-LSTM was formulated based on the Long Short-Term Memory (LSTM) approach. The investigation also delved into assessing the influence of the number of hidden units (2, 4, 8, 16, 32, 64, 128, 256, and 512) and the number of inputs (for one-step, five-step, ten-step, and twenty-step predictions) on the efficacy of the proposed model. Specifically, the structure of this paper is organized as follows, Section 1 serves as the Introduction, primarily introducing the research background, significance, and the current research status both domestically and internationally. Section 2 is dedicated to Methodology, detailing the wavelet decomposition method, the LSTM model, and the method proposed in this paper. Section 3 presents a case study, focusing on the bridge health monitoring system and examining the impact of the number of input parameters and the choice of wavelet functions on prediction performance and computational time. Section 4 concludes the paper by summarizing the constructed models and proposing the optimal model

structure.

2. Methodology

2.1 Wavelet decomposition method

Sequence data, particularly monitoring data, often exhibits waveform characteristics, while real-time sequence data demonstrates repeatability characteristics (Sandham *et al*. 1998). Consequently, sequence data can be effectively represented by "infinite" waveform functions. The wavelet decomposition (WD) method, as described by Wang *et al*. (2006), is utilized to progressively decompose the monitoring data into high and low frequencies. This decomposition is accomplished by employing wavelet functions to analyze the time series data.

$$\begin{aligned} &\psi(t) = \frac{1}{\sqrt{a}}\psi\left(\frac{t-b}{a}\right) \\ &a = 2^j \\ &b = k2^j \end{aligned} \tag{1}$$

where t is the time; a is the scale factor; b is the translation factor; j is the scale coefficient; k is the translation coefficient.

Through establishing a threshold T for the wavelet coefficients as detailed earlier, the high-frequency data within the monitoring data can be sieved out, efficiently eradicating noise information present in wavelet functions surpassing the threshold. In wavelet de-noising methods, Bayesian threshold, Stein's Unbiased Risk Estimator (SURE) threshold, and Minmax threshold are three commonly used methods. Bayesian threshold can adaptively select thresholds based on the statistical characteristics of signals, such as noise levels, which helps to achieve better denoising effects under different signal conditions. Especially when the noise level is high, Bayesian threshold method can more effectively suppress noise. However, compared to other threshold selection methods, Bayesian threshold requires a larger amount of computation and increases processing time. Com-pared to Bayesian threshold, the SURE threshold method based on unbiased risk estimation principle has lower computational complexity and is simpler to implement. However, its denoising effect may be affected by signal characteristics, and parameters may need to be adjusted for different types of signals to achieve optimal results. The Minmax threshold method is based on the principle of minimizing maximum error and has good robustness, which can maintain stable denoising effects at different noise levels. However, the denoising effect of Minmax threshold may be affected by parameter settings and needs to be adjusted to achieve the best results.

The SURE threshold estimation method computes the threshold T of wavelet coefficients based on the unbiased likelihood estimation criterion, as demonstrated in Benaouda *et al*. (2006).

$$\begin{aligned} &R(T) = \sum_{i=1}^{N}(\min(|y_i|,T))^2 + \sigma_n^2 - \frac{2\sigma_n^2}{N}\sum_{i=1}^{N} I\left(|y_i| \le T\right) \\ &T = \arg\min R(T) \end{aligned} \tag{2}$$

The Bayesian threshold estimation method models the wavelet function based on statistical characteristics and then obtains the threshold T through Bayesian estimation, as illustrated in Hashemi and Beheshti (2009).

$$T = \frac{\sigma_n^2}{\sigma_w} \tag{3}$$

The Minmax threshold estimation method calculates the wavelet function to obtain the threshold T based on the maximum minimization principle, as described by Janeiro and Ramos (2018).

$$T = \begin{cases} 0 & N \le 32 \\ 0.3936 + \dfrac{0.1829 \lg N}{\lg 2} & N \le 32 \end{cases} \tag{4}$$

where N is the number of wavelet function layers; σ_n is the standard deviation of noise; σ_w is the standard deviation of the initial wavelet function; I is the judgment function.

2.2 WD-LSTM prediction model

Long and Short-term Memory (LSTM) is a cyclic neural network that can analyze input information based on time series, as discussed by Meng *et al*. (2020). In other words, it considers the correlation between input information at the current time and input information at the next time, as highlighted by Cao (2024) and Yuan *et al*. (2021). Typically, an LSTM network consists of input gates, forget gates, and output gates, as shown in Fig. 1. The input gate saves the input information to the cell and creates a new state vector. The forget gate stores the hidden state information of the previous cell into the current cell. And the output gate outputs the cell state information to the next cell, as explained by Xu *et al*. (2021).

In Fig. 1., the i is the input gate, and its weight and offset are i_t and b_i respectively; f is the forgetting gate, and its weight and offset are f_t and b_f respectively; o is the output gate, and its weight and offset are o_t and b_o respectively; x_t is unit input; z_t is the status of temporary unit; c_t is the current unit state; $c_{t\text{-}1}$ is the status of the previous unit; h_t is the hidden state of the current unit; $h_{t\text{-}1}$ is the hidden state of the previous unit. Specially, they can be expressed by (Ding *et al*. 2023f, Zhang *et al*. (2019))

$$f_t = sigmoid\left(W_f \times [h_{t-1}, x_t] + b_f\right) \tag{5}$$

$$i_t = sigmoid(W_i \times [h_{t-1}, x_t] + b_i) \tag{6}$$

$$o_t = sigmoid(W_o \times [h_{t-1}, x_t] + b_o) \tag{7}$$

$$z_t = tanh(W_z \times [h_{t-1}, x_t] + b_z) \tag{8}$$

$$c_t = (c_{t-1} \otimes f_t) \oplus (z_t \otimes i_t) \tag{9}$$

$$h_t = tanh(c_t) \otimes o_t \tag{10}$$

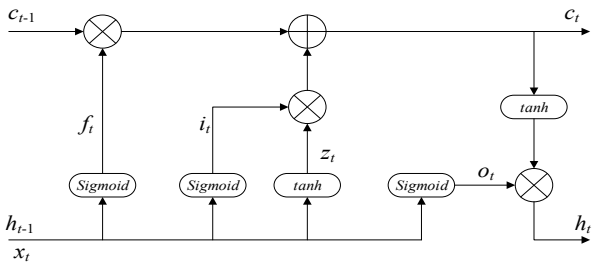

Fig. 1 LSTM network

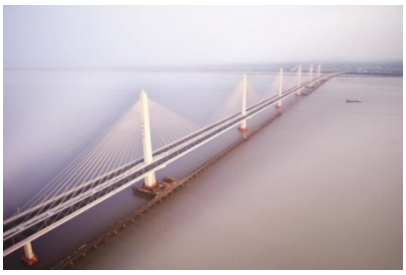

Fig. 2 Investigated bridge

Therefore, the WD method is used to denoise the data in order to improve data quality at first. Then, the denoised data is modeled and predicted using the LSTM network. The main advantage of the proposed model, called WD-LSTM, lies in its combination of WD denoising and the LSTM network. This combination enables better handling of the temporal characteristics of time series data and accurate prediction of future values. Specially, the processed wind speed data is divided into a training set and a test set, with the training set accounting for 90% of the dataset and the test set accounting for 10%. The input/output data structure is time series data. The learning rate controls the speed of parameter updates; if it is too large, the model may fail to converge, while if it is too small, the training process may be slow. The number of iterations affects the efficiency and stability of model training. In this paper, the learning rate is set to 0.005, the number of iterations is 100, the sigmoid function is selected as the activation function to control information forgetting, input, and output generation, and the Adam optimization algorithm is chosen to optimize model parameters during the training process.

2.3 WD-LSTM prediction model

In order to evaluate the prediction performance of the model, the root mean square error (RMSE) is used to assess the performance of wind speed prediction model, that is, (Ding *et al*. (2024c))

$$RMSE = \sqrt{\frac{1}{N}\sum_{t=1}^{N}(y_i - f_i)^2} \tag{11}$$

R^2 is a statistical measure of how well the model predictions approximate the observation data points (Nagelkerke 1991). It is expressed as

$$R^2 = 1 - \frac{\sum_i (y_i - f_i)^2}{\sum_i (y_i - \bar{y})^2} \tag{12}$$

where y_i is the ith observation data point; f_i is the ith corresponding model prediction; $\bar{y}$ is the mean of the observation data; and N is total observation data. As can be seen from the definition of the RMSE rule, the smaller the RMSE value, the better the fit of the model. Unlike the RMSE, the larger the R^2 value, the better the prediction performance of the model.

3. Illustrative application: Jiashao Bridge

3.1 Bridge description and SHM

The Jiashao Bridge, situated in Hangzhou Bay, Zhejiang Province, China, extends from Guzhu Junction in the south, linking the Chang-Tai Expressway (Shang-San Expressway) and Hang-Ningbo Expressway, to Nanhu Junction in the north, connecting with Zhajia-su Expressway, a section of Chang-tai Expressway (National Highway G1522), as depicted in Fig. 2. Configured as a cable-stayed bridge, the Jiashao Bridge spans a total length of 10.137 km (Ding *et al*. 2023g). Despite being one-third the length of the Hangzhou Bay Sea-crossing Bridge, the Jiashao Bridge features a broader deck, measuring 40.5 meters, with its main bridge extending 2,680 meters in length. Comprising five continuous segments, each equipped with six towers, every individual span measures 428 meters.

To accurately monitor the surrounding ambient winds near the Jiashao Bridge, a Structural Health Monitoring (SHM) system was installed, incorporating an ultrasonic anemometer (UAN-G54-001-1). This ultrasonic anemometer operates at a sampling frequency of 10 Hz, covering a wind speed range from 0 to 60 m/s, and ensuring a resolution of 0.01 m/s for precise measurements. The positioning of the ultrasonic anemometer on the Jiashao Bridge is illustrated in Fig. 3. Specially, in order to avoid interference from low wind speed areas below the ground and bridge structures on the measurement results, wind speed and direction sensors should be installed at a sufficiently high position. Based on this, wind speed and direction sensors are installed on the Jiashao Bridge at a horizontal distance of 4 m from the bridge deck, with a height of 1 m. Wind data obtained in December 2020 were utilized to characterize the wind patterns. Specifically, the ultrasonic anemometer collected ten wind speed readings per second, and for this study, the maximum wind speed recorded over a ten-minute duration was selected (Ding *et al*. 2023h).

3.2 Influence of wavelet threshold for wind speed prediction

In order to reduce the sources of uncertainty in the health monitoring system for large-span bridge structures and ensure the accuracy of wind speed data collection. Firstly, the bridge structure health monitoring system consists of high-precision and high stability wind speed and

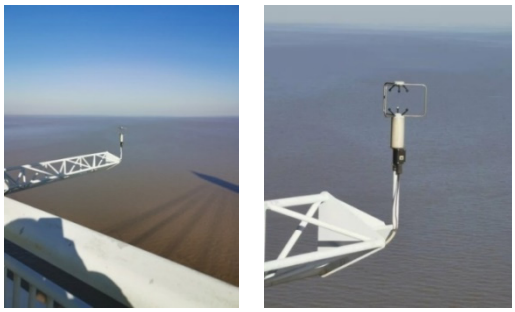

Fig. 3 Deployment of wind anemometers on investigated bridge

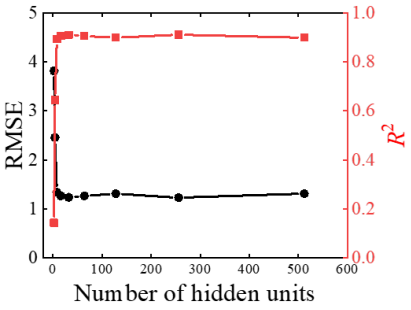

Fig. 5 Influence of the number of hidden units on one-step prediction performance with SURE threshold

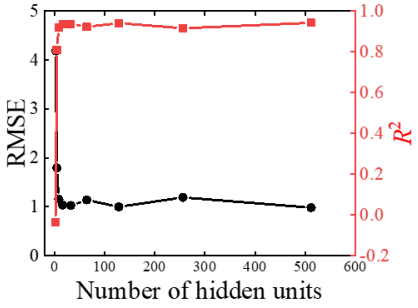

Fig. 4 Influence of the number of hidden units on one-step prediction performance with Bayesian threshold

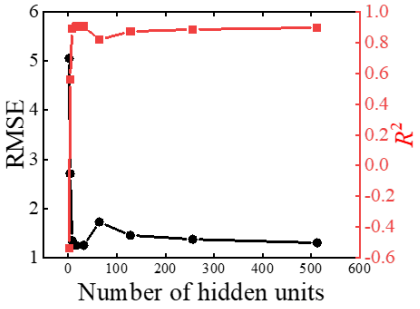

Fig. 6 Influence of the number of hidden units on one-step prediction performance with Bayesian threshold

direction sensors, namely ultrasonic sensors. Its measurement accuracy and stability are usually better than mechanical sensors, and it is less affected by environmental factors. Secondly, the wavelet denoising method is used to preprocess the original monitoring data by filtering and denoising, in order to improve the accuracy and re-liability of the data. Specially, the wind speed data underwent denoising using the Bayesian threshold method. Subsequently, an LSTM prediction model was developed for one-step prediction. The model was trained with a learning rate of 0.005 over 100 iterations. An analysis was conducted to assess the impact of different numbers of hidden units (ranging from 2 to 512) on wind speed prediction performance, as illustrated in Fig. 4. The findings indicated that the LSTM model demonstrated the most effective prediction performance with 32 hidden units, resulting in an RMSE value of 1.0244 and an R^2 value of 0.93802.

After denoising the wind speed data using the SURE threshold method, an LSTM prediction model was constructed for one-step prediction, employing a single input and single output. The analysis, depicted in Fig. 5, focused on examining the effects of different numbers of hidden units on wind speed prediction performance. The results highlighted that the LSTM model attained its optimal prediction performance with 32 hidden units, yielding an RMSE value of 1.23634 and an R^2 value of 0.9102.

Following denoising using the Minmax threshold method, an LSTM prediction model was established for one-step prediction, employing a single input and single output. The investigation, detailed in Fig. 6, aimed to explore the influence of varying numbers of hidden units on wind speed prediction performance. The results demonstrated that the LSTM model delivered its optimal prediction performance with 32 hidden units, yielding an RMSE value of 1.25289 and an R^2 value of 0.90554.

The LSTM model's prediction performance shows gradual improvement as the number of hidden units increases, allowing for more effective training and fitting. However, an excessive number of hidden units can lead to overfitting, causing fluctuations in prediction performance. Consequently, for one-step prediction, the optimal number of hidden units in the LSTM model is determined to be 32. Additionally, the LSTM model, based on the Bayesian threshold, outperforms the SURE and Minmax threshold approaches in terms of prediction performance. The one-step prediction results of the LSTM model using the Bayesian threshold are depicted in Fig. 7. As shown in Fig. 7(a), the LSTM model accurately captures the wind speed trend. Furthermore, Fig. 7(b) demonstrates that the LSTM model's predicted wind speed closely aligns with the measured wind speed, exhibiting minimal error.

3.3 Influence of input numbers for wind speed prediction

Utilizing the Bayesian threshold denoising method, an LSTM prediction model was constructed for multi-step prediction using a multi-input and single-output approach. In the context of a five-step prediction, the LSTM model demonstrated its peak performance with 64 hidden units, resulting in an RMSE value of 0.6454 and an R^2 value of 0.97555, as illustrated in Fig. 8. Examination of Fig. 8 indicates that as the number of hidden units in the LSTM model increased from 2 to 64, there was a discernible

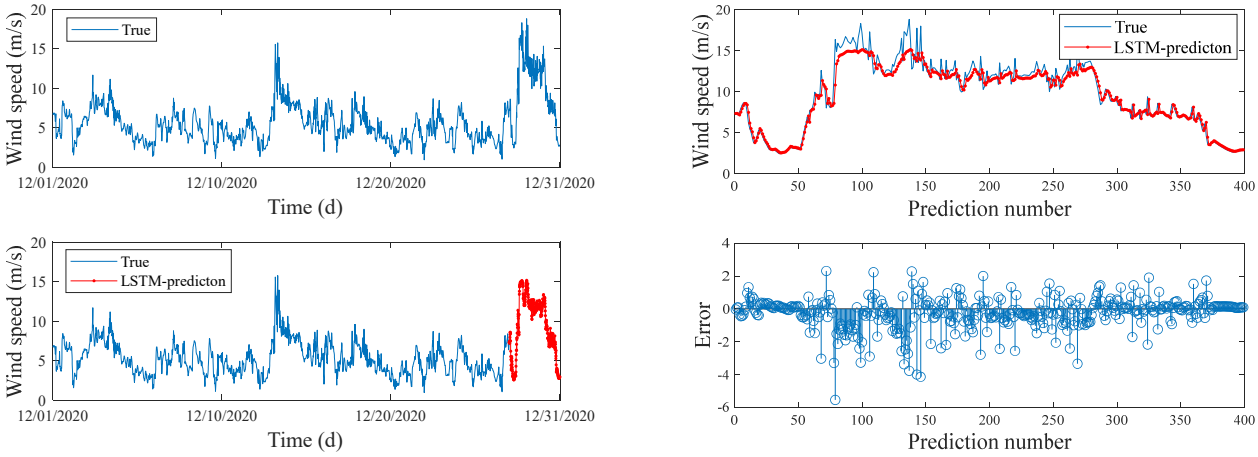

(a) Prediction trend of wind speed

(b) Prediction results of wind speed

Fig. 7 One-step prediction results of LSTM model with Bayesian threshold

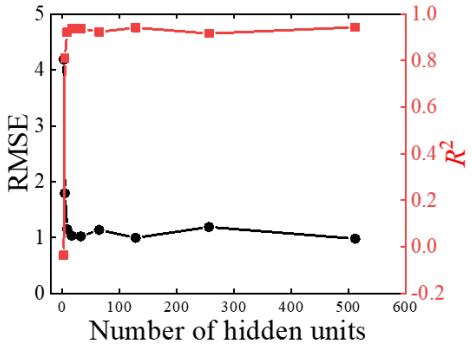

Fig. 8 Influence of the number of hidden units on five-step prediction performance

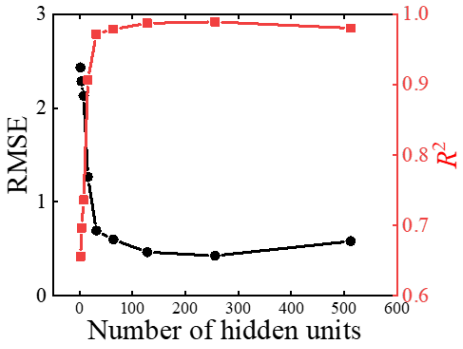

Fig. 9 Influence of the number of hidden units on ten-step prediction performance

decrease in the RMSE value alongside a substantial increase in the R^2 value. This observation suggests that the number of hidden units significantly influences the predictive performance of the model. However, beyond a certain threshold, further increases in the number of hidden units do not lead to significant improvements in predictive performance. This implies the presence of a non-linear relationship between the number of hidden units and the model's predictive performance, characterized by a turning point. In this investigation, the optimal number of hidden units was determined to be 64.

For a ten-step prediction, the LSTM model demonstrated its optimal predictive performance with 128 hidden units, yielding an RMSE value of 0.46523 and an R^2 value of 0.98744, as depicted in Fig. 9. Specifically, the figure illustrates that as the number of hidden units in the LSTM model escalates from 2 to 128, the RMSE value decreases rapidly, while the R^2 value increases significantly. This pattern indicates that the number of hidden units notably influences the model's predictive performance. However, beyond a certain threshold, augmenting the number of hidden units does not result in substantial improvements in the model's predictive performance. Hence, a non-linear relationship exists between the number of hidden units and the model's predictive performance, characterized by a threshold. In this specific scenario, the optimal number of hidden units was determined to be 128.

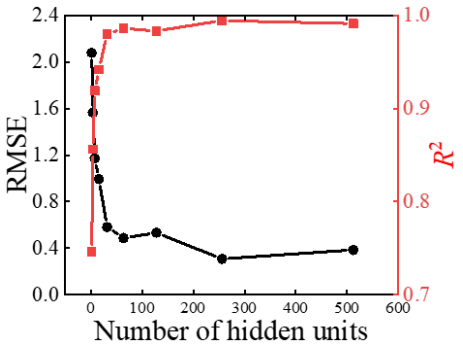

Fig. 10 Influence of the number of hidden units on twenty-step prediction performance

For a twenty-step prediction, the LSTM model showcased exceptional predictive performance with 256 hidden units, yielding an RMSE value of 0.46523 and an R^2 value of 0.98744, as shown in Fig. 10. The figure unmistakably demonstrates that as the number of hidden units in the LSTM model increases from 2 to 256, the RMSE value decreases rapidly, while the R^2 value increases significantly. This pattern indicates a substantial influence of the number of hidden units on the model's predictive performance. However, beyond a certain threshold,

augmenting the number of hidden units does not result in significant improvements in the model's predictive performance. Consequently, a non-linear relationship exists between the number of hidden units and the model's predictive performance, characterized by a noticeable threshold. In this specific case, the optimal number of hidden units was determined to be 256.

As expected, there is a noticeable enhancement in wind speed prediction accuracy as the number of inputs increases, attributed to the strong correlation between the subsequent wind speed and historical wind speed data. Moreover, a higher number of inputs also corresponds to an optimal number of hidden units for the LSTM prediction model. However, it's crucial to recognize that an increase in the number of inputs and hidden units results in extended computational time for both model training and prediction, as illustrated in Fig. 11. All computations were conducted on a computer system equipped with an Intel® Core™ i5-8300H CPU @2.30GHz processor running at 2.30 GHz, operating on a 64-bit system. Specifically, LSTM model-1, entailing a one-step prediction of LSTM with 32 hidden units, necessitated 34 seconds for computation. LSTM model-2, a five-step prediction of LSTM with 64 hidden units, demanded 72 seconds. LSTM model-3, involving a ten-step prediction of LSTM with 128 hidden units, took 200 seconds to compute. Lastly, LSTM model-4, a twenty-step prediction of LSTM with 256 hidden units, required 577 seconds. Therefore, while emphasizing prediction accuracy, it's equally vital to consider the computational time. Based on these findings, it is advisable to employ LSTM model-2, encompassing a five-step prediction of LSTM with 64 hidden units, for wind speed prediction.

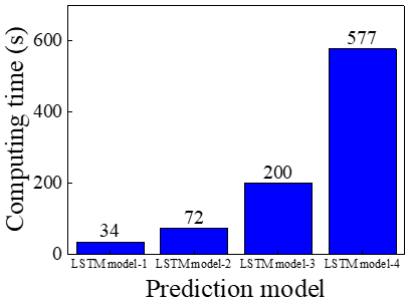

Fig. 11 Comparison of calculation time of prediction model

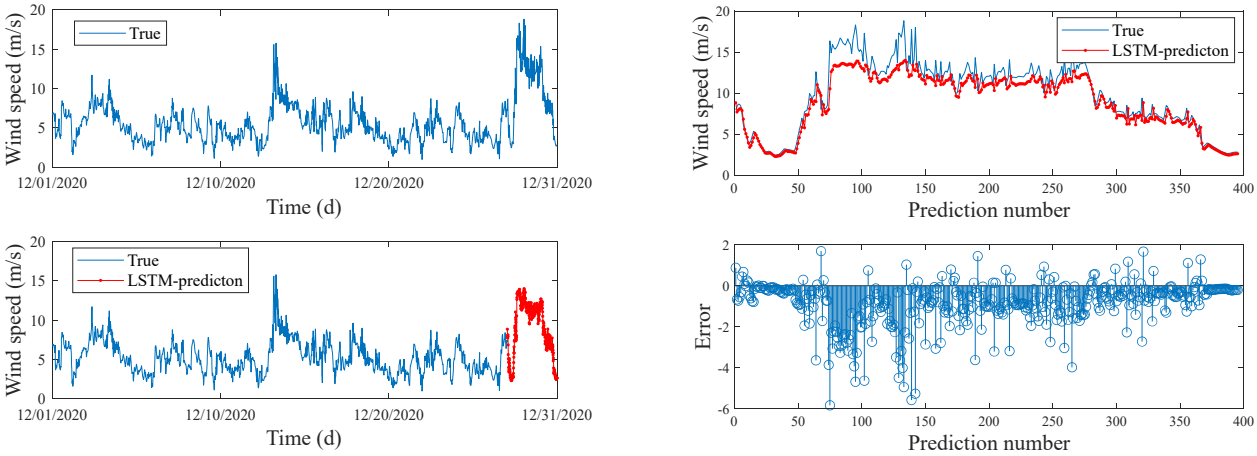

(a) Prediction trend of wind speed (b) Prediction results of wind speed

Fig. 12 Five-step prediction results of LSTM model with Bayesian threshold

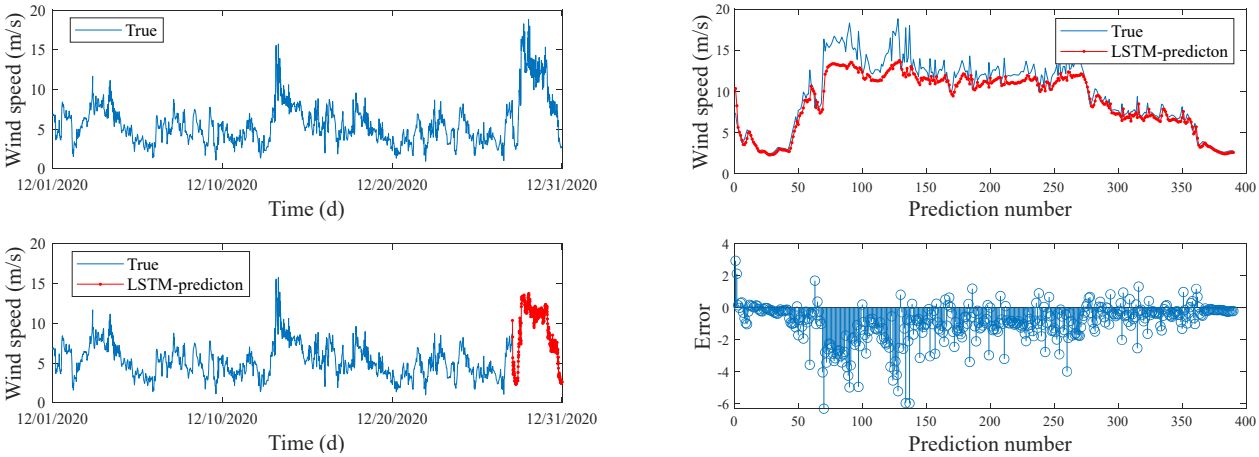

(a) Prediction trend of wind speed (b) Prediction results of wind speed

Fig. 13 Ten-step prediction results of LSTM model with Bayesian threshold

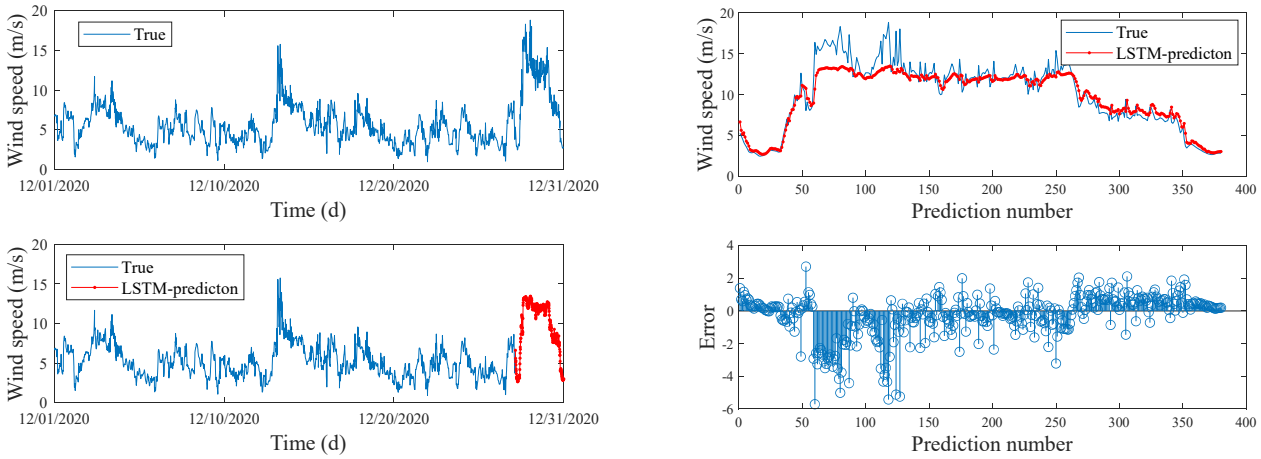

(a) Prediction trend of wind speed

(b) Prediction results of wind speed

Fig. 14 Twenty-step prediction results of LSTM model with Bayesian threshold

The outcomes of the LSTM model's five-step prediction, utilizing the Bayesian threshold, are presented in Fig. 12. Fig. 12(a) clearly demonstrates that the developed WD-LSTM model effectively anticipates the trend of wind speed fluctuations, showcasing the model's ability to accurately predict wind speed even in the presence of pronounced random characteristics. Additionally, Fig. 12(b) delineates the specific disparities between the predicted wind speed and the actual measured wind speed. The average wind speed prediction error nearly approximates 0 m/s, with a maximum prediction error of 6 m/s. This is primarily due to substantial wind speed variations between the 50th and 150th predictions, underscoring the significant uncertainty associated with wind speed. While the WD-LSTM model exhibits relatively larger prediction errors at certain junctures, overall, the model demonstrates commendable predictive performance.

The predictions for a ten-step horizon using the LSTM model based on the Bayesian threshold are depicted in Fig. 13. In Fig. 13(a), it is evident that the developed WD-LSTM model adeptly captures the wind speed trends, showcasing its capability to accurately forecast wind speed even in the presence of substantial random characteristics. Furthermore, Fig. 13(b) outlines the specific variances between the predicted wind speed and the actual measured wind speed. Notably, the average wind speed prediction error approximates 0 m/s, with a maximum prediction error of 6 m/s, predominantly occurring between the 50th and 150th predictions, emphasizing the inherent uncertainty linked with wind speed. While the WD-LSTM model may display relatively larger prediction errors at specific instances, overall, the model demonstrates commendable predictive performance.

The results of the twenty-step wind speed predictions using the LSTM model based on the Bayesian threshold approach are depicted in Fig. 14. As illustrated in Fig. 14(a), it is evident that the developed WD-LSTM model adeptly forecasts the trends in wind speed changes, showcasing its capacity to make accurate wind speed predictions, even in the presence of notable random characteristics. Furthermore, Fig. 14(b) provides insights into the specific variations between the predicted wind speed and the actual measured wind speed. The average wind speed prediction error hovers around 0 m/s, with the maximum prediction error reaching 6 m/s, primarily stemming from substantial wind speed variations between the 50th and 150th predictions, highlighting the inherent uncertainty associated with wind speed. Although the WD-LSTM model may exhibit larger prediction errors at specific instances, overall, it demonstrates favorable predictive performance. From the aforementioned case study, it becomes evident that with an increase in the number of input parameters (one-step, five-step, ten-step, and twenty-step), the optimal number of hidden layers also gradually rises. This underscores that in a multi-input, single-output model, the number of hidden layers and units significantly influence the predictive performance of the model.

4. Conclusions

This study introduces the WD-LSTM wind speed prediction model and investigates the effects of Bayesian threshold, SURE threshold, and Minmax threshold in WD on prediction performance. Additionally, the research explores the impact of varying numbers of hidden units (2, 4, 8, 16, 32, 64, 128, 256, and 512) and inputs (one-step, five-step, ten-step, and twenty-step) in WD-LSTM on prediction performance. The proposed WD-LSTM prediction models, featuring diverse hidden units and inputs, are validated using SHM data. Furthermore, the computational time of WD-LSTM prediction models with different hidden units and inputs is compared. The principal conclusions derived from the study are as follows:

(1) The proposed WD-LSTM model presents a viable approach for wind speed prediction and demonstrates impressive prediction performance, as confirmed by SHM data.
(2) The LSTM model, utilizing the Bayesian threshold, surpasses those employing SURE and Minmax thresholds in terms of prediction accuracy.
(3) Increasing the number of inputs enhances prediction

accuracy, but it requires more hidden units, emphasizing the significant relationship between the wind speed at the next moment and historical wind speed.

(4) As the number of inputs and hidden units increases, the computation time for training and prediction of the WD-LSTM model also increases. Therefore, it is crucial to consider computation time while ensuring prediction accuracy.

(5) The future trend and technology of wind monitoring for large-span bridges will mainly focus on improving monitoring accuracy, intelligence level, and effective utilization of data. On the one hand, developing high-precision sensor technology enables more accurate capture of small changes in parameters such as wind speed and direction, providing more precise data support for the safety assessment of bridges. On the other hand, through big data technology and artificial intelligence technology, massive monitoring data can be deeply mined and analyzed to reveal the laws and characteristics of bridge wind loads.

Acknowledgments

The work described in this paper was jointly supported by the State Key Laboratory of Mountain Bridge and Tunnel Engineering (Grant No. SKLBT-2210), the National Natural Science Foundation of China (Grant No. 52408349), the Zhejiang Provincial Natural Science Foundation of China (Grant No. LQN25E080020), the National Statistical Research Program (Grant No. 2024LZ001), the Ministry of Education of Humanities and Social Science Project (Grant No. 23YJCZH037), the Key Laboratory of C&PC Structures, Ministry of Education (Grant No. CPCSME2024-01), and the Fundamental Research Funds for the Central Universities, CHD (Grant No. JQJJ202404).

References

An, X., Jiang, D., Liu, C. and Zhao, M. (2011), "Wind farm power prediction based on wavelet decomposition and chaotic time series", *Expert Syst. Appl.*, **38**(9), 11280-11285. https://doi.org/10.1016/j.eswa.2011.02.176

Benaouda, D., Murtagh, F., Starck, J.L. and Renaud, O. (2006), "Wavelet-based nonlinear multiscale decomposition model for electricity load forecasting", *Neurocomputing*, **70**(1-3), 139-154. https://doi.org/10.1016/j.neucom.2006.04.005

Cadenas, E. and Rivera, W. (2010), "Wind speed forecasting in three different regions of Mexico, using a hybrid ARIMA-ANN model", *Renew. Energy*, **35**(12), 2732-2738. https://doi.org/10.1016/j.renene.2010.04.022

Cao, Y.J. (2024), "Research on prediction of deformation value of the foundation pit based on bayesian and LSTM neural network models", *J. Muni. Tech.*, **42**(11), 119-126. [In Chinese] https://doi.org/10.19922/j.1009-7767.2024.11.119

Chen, K. and Yu, J. (2014), "Short-term wind speed prediction using an unscented Kalman filter based state-space support vector regression approach", *Appl. Energy*, **113**, 690-705. https://doi.org/10.1016/j.apenergy.2013.08.025

Cui, W., Ma, T., Zhao, L. and Ge, Y. (2021), "Data-based windstorm type identification algorithm and extreme wind speed prediction", *J. Struct. Eng.*, **147**(5), 04021053. https://doi.org/10.1061/(ASCE)ST.1943-541X.0002954

Ding, J., Chen, G., Huang, Y., Zhu, Z., Yuan, K. and Xu, H. (2021), "Short-term wind speed prediction based on CEEMDAN-SE-improved PIO-GRNN model", *Measur. Contr.*, **54**(1-2), 73-87. https://doi.org/10.1177/0020294020981400

Ding, Y., Ye, X.W., Guo, Y., Zhang, R. and Ma, Z. (2023a), "Probabilistic method for wind speed prediction and statistics distribution inference based on SHM data-driven", *Proba. Eng. Mech.*, **73**, 103475. https://doi.org/10.1016/j.probengmech.2023.103475

Ding, Y., Ye, X.W. and Guo, Y. (2023b), "Copula-based JPDF of wind speed, wind direction, wind angle and temperature with SHM data", *Proba. Eng. Mech.*, 103483. https://doi.org/10.1016/j.probengmech.2023.103483

Ding, Y., Ye, X.W. and Su, Y.H. (2023c), "A framework of cable wire failure mode deduction based on Bayesian network", *Structures*, **57**, 104996. https://doi.org/10.1016/j.istruc.2023.104996

Ding, Y., Hang, D., Wei, Y.J., Zhang, X.L., Ma, S.Y., Liu, Z.X., Zhou, S.X. and Han, Z. (2023d), "Settlement prediction of existing metro induced by new metro construction with machine learning based on SHM data: a comparative study", *J. Civil Struct. Health Monitor.*, **13**(6-7), 1447-1457. https://doi.org/10.1007/s13349-023-00714-4

Ding, Y., Ye, X.W., Ding, Z., Wei, G., Cui, Y.L., Han, Z. and Jin, T. (2023e), "Short-term tunnel-settlement prediction based on Bayesian wavelet: a probability analysis method", *J. Zhejiang Univ. Sci. A*, **24**(11), 960-977. https://doi.org/10.1631/jzus.A2200599

Ding, Y., Ye, X.W. and Guo, Y. (2023f), "A multi-step direct and indirect strategy for predicting wind direction based on EMD-LSTM model", *Struct. Control Health Monitor.*, 4950487. https://doi.org/10.1155/2023/4950487

Ding, Y., Ye, X.W. and Guo, Y. (2023g), "Data set from wind, temperature, humidity and cable acceleration monitoring of the Jiashao bridge", *J. Civil Struct. Health Monitor.*, **13**(3), 579-589. https://doi.org/ 10.1007/s13349-022-00662-5

Ding, Y., Ye, X.W. and Guo, Y. (2023h), "Wind load assessment with the JPDF of wind speed and direction based on SHM data", *Structures*, **47**(1), 2074-2080. https://doi.org/10.1016/j.istruc.2022.12.028

Ding, Y., He, Z.X. and Zhou, S.X. (2024a), "Multi-dimensional models for predicting the chloride diffusion in concrete exposed to marine tidal zone: Methodology, Numerical Simulation and Application", *Comput. Concrete, Int. J.*, **34**(2), 169-178. https://doi.org/10.12989/cac.2024.34.2.169

Ding, Y., Ye, X.W., Zhang, H. and Zhang, X.S. (2024b), "Fatigue life evolution of steel wire considering corrosion-fatigue coupling effect: Analytical model and application", *Steel Compos. Struct., Int. J.*, **50**(3), 363-374. https://doi.org/10.12989/scs.2024.50.3.363

Ding, Y., Wei, Y.J., Xi, P.S., Ang, P.P. and Han, Z. (2024c), "A long-term tunnel settlement prediction model based on BO-GPBE with SHM data", *Smart Struct. Syst., Int. J.*, **33**(1), 17-26. https://doi.org/10.12989/sss.2024.33.1.017

Ding, Y., Ye, X.W. and Su, Y.H. (2025), "Wind-induced fatigue life prediction of bridge hangers considering the effect of wind direction", *Eng. Struct.*, **327**, 119523. https://doi.org/10.1016/j.engstruct.2024.119523

Fenerci, A., Øiseth, O. and Rønnquist, A. (2017), "Long-term monitoring of wind field characteristics and dynamic response of a long-span suspension bridge in complex terrain", *Eng. Struct.*, **147**, 269-284. https://doi.org/10.1016/j.engstruct.2017.05.070

Hashemi, M. and Beheshti, S. (2009), "Adaptive noise variance estimation in BayesShrink", *IEEE Signal Proc. Lett.*, **17**(1), 12-15. https://doi.org/10.1109/LSP.2009.2030856

Janeiro, F.M. and Ramos, P.M. (2018), "Threshold estimation for least-squares fitting in impedance spectroscopy", *Measurement*, **124**, 479-485. https://doi.org/10.1016/j.measurement.2018.04.071

Joseph, L.P., Deo, R.C., Prasad, R., Salcedo-Sanz, S., Raj, N. and Soar, J. (2023), "Near real-time wind speed forecast model with bidirectional LSTM networks", *Renew. Energy*, **204**, 39-58. https://doi.org/10.1016/j.renene.2022.12.123

Li, H., Ou, J., Zhao, X., Zhou, W., Li, H., Zhou, Z. and Yang, Y. (2006), "Structural health monitoring system for the Shandong Binzhou Yellow River highway bridge", *Comput.-Aided Civil Infrastruct. Eng.*, **21**(4), 306-317. https://doi.org/10.1111/j.1467-8667.2006.00437.x

Li, Y., Zhu, L., Qian, C., Jian, X. and Sun, L. (2021), "The time-varying modal information of a cable-stayed bridge: Some consideration for SHM", *Eng. Struct.*, **235**, 111835. https://doi.org/10.1016/j.engstruct.2020.111835

Liu, H., Tian, H.Q. and Li, Y.F. (2012), "Comparison of two new ARIMA-ANN and ARIMA-Kalman hybrid methods for wind speed prediction", *Appl. Energy*, **98**, 415-424. https://doi.org/10.1016/j.apenergy.2012.04.001

Liu, H., Tian, H.Q. and Li, Y.F. (2015), "An EMD-recursive ARIMA method to predict wind speed for railway strong wind warning system", *J. Wind Eng. Ind. Aerodyn.*, **141**, 27-38. https://doi.org/10.1016/j.jweia.2015.02.004

Liu, M.D., Ding, L. and Bai, Y.L. (2021), "Application of hybrid model based on empirical mode decomposition, novel recurrent neural networks and the ARIMA to wind speed prediction", *Energy Conv. Manag.*, **233**, 113917. https://doi.org/10.1016/j.enconman.2021.113917

Lim, J.Y., Kim, S., Kim, H.K. and Kim, Y.K. (2022), "Long short-term memory (LSTM)-based wind speed prediction during a typhoon for bridge traffic control", *J. Wind Eng. Ind. Aerodyn.*, **220**, 104788. https://doi.org/10.1016/j.jweia.2021.104788

López, G. and Arboleya, P. (2022), "Short-term wind speed forecasting over complex terrain using linear regression models and multivariable LSTM and NARX networks in the Andes Mountains, Ecuador", *Renew. Energy*, **183**, 351-368. https://doi.org/10.1016/j.renene.2021.10.070

Meng, X., Fu, H., Peng, L., Liu, G., Yu, Y., Wang, Z. and Chen, E. (2020), "D-LSTM: short-term road traffic speed prediction model based on GPS positioning data", *IEEE Trans. Intell. Transp. Syst.*, **23**(3), 2021-2030. https://doi.org/10.1109/TITS.2020.3030546

Mishra, M., Dash, P.B., Nayak, J., Naik, B. and Swain, S.K. (2020), "Deep learning and wavelet transform integrated approach for short-term solar PV power prediction", *Measurement*, **166**, 108250. https://doi.org/10.1016/j.measurement.2020.108250

Nagelkerke, N.J.D. (1991), "A note on a general definition of the coefficient of determination", *Biometrika*, **78**(3), 691-692. https://doi.org/10.1093/biomet/78.3.691

Park, J., Jung, J., Park, S. and Yoon, H. (2023), "Automated structural modal analysis method using long short-term memory network", *Smart. Struct. Syst., Int. J.*, **31**(1), 45-56. https://doi.org/10.12989/sss.2023.31.1.045

Sareen, K., Panigrahi, B.K., Shikhola, T. and Sharma, R. (2023), "An imputation and decomposition algorithms based integrated approach with bidirectional LSTM neural network for wind speed prediction", *Energy*, **278**, 127799. https://doi.org/10.1016/j.energy.2023.127799

Sandham, W., Hamilton, D., Fisher, A., Xu, W. and Conway, M. (1998), "Multiresolution wavelet decomposition of the seismocardiogram", *IEEE Trans. Signal Process.*, **46**(9), 2541-2543. https://doi.org/10.1109/78.709542

Santos, V.O., Rocha, P.A.C., Scott, J., Thé, J.V.G. and Gharabaghi, B. (2023), "Spatiotemporal analysis of bidimensional wind speed forecasting: Development and thorough assessment of LSTM and ensemble graph neural networks on the Dutch database", *Energy*, **278**, 127852. https://doi.org/10.1016/j.energy.2023.127852

Salehi Borujeni, M., Dideban, A. and Akbari Foroud, A. (2021), "Reconstructing long-term wind speed data based on measure correlate predict method for micro-grid planning", J. Ambient Intell. Humaniz. Comput., 12(11), 10183-10195. https://doi.org/10.1007/s12652-020-02784-4

Son, H., Yoon, C., Kim, Y., Jang, Y., Tran, L.V., Kim, S.E. and Park, J. (2022), "Damaged cable detection with statistical analysis, clustering, and deep learning models", *Smart Struct. Syst., Int. J.*, **29**(1), 17-28. https://doi.org/10.12989/sss.2022.29.1.017

Ti, Z., Zhang, M., Li, Y. and Wei, K. (2019), "Numerical study on the stochastic response of a long-span sea-crossing bridge subjected to extreme nonlinear wave loads", *Eng. Struct.*, **196**, 109287. https://doi.org/10.1016/j.engstruct.2019.109287

Wang, M. and Van Der Schaar, M. (2006), "Operational rate-distortion modeling for wavelet video coders", *IEEE Trans. Signal Process.*, **54**(9), 3505-3517. https://doi.org/10.1109/TSP.2006.879273

Wang, S., Zhang, N., Wu, L. and Wang, Y. (2016), "Wind speed forecasting based on the hybrid ensemble empirical mode decomposition and GA-BP neural network method", *Renew. Energy*, **94**, 629-636. https://doi.org/10.1016/j.renene.2016.03.103

Wang, L., Li, X. and Bai, Y. (2018), "Short-term wind speed prediction using an extreme learning machine model with error correction", *Energy Conv. Manag.*, **162**, 239-250. https://doi.org/10.1016/j.enconman.2018.02.015

Wang, K., Li, K., Zhou, L., Hu, Y., Cheng, Z., Liu, J. and Chen, C. (2019), "Multiple convolutional neural networks for multivariate time series prediction", *Neurocomputing*, **360**, 107-119. https://doi.org/10.1016/j.neucom.2019.05.023

Wang, X.H., Shi, Y., Shen, X.W., Chen, Y.J., Zhang, H.F. and Shi, J. (2024a), "Wave parameter downscaling forecasting model based on random forest algorithm", *J. Changsha Univ. Sci. Tech.* (*Nat. Sci.*), 1-9. [In Chinese] https://doi.org/10.19951/j.cnki.1672-9331. 20240508002

Wang, F.Z., Ren, Y.L, Zhang, L. and Wang, D. (2024b), "Fault diagnosis of bidirectional DC-DC power converter based on improved LSTM-SVM", *J. Henan Poly. Univ.* (*Nat. Sci.*), **43**(5), 118-126. [In Chinese] https://doi.org/10.16186/j.cnki.1673-9787.2022060019

Xu, Y.L. and Chen, J. (2004), "Characterizing nonstationary wind speed using empirical mode decomposition", *J. Struct. Eng.*, **130**(6), 912-920. https://doi.org/10.1061/(ASCE)0733-9445(2004)130:6(912)

Xu, W., Liu, P., Cheng, L., Zhou, Y., Xia, Q., Gong, Y. and Liu, Y. (2021), "Multi-step wind speed prediction by combining a WRF simulation and an error correction strategy", *Renew. Energy*, **163**, 772-782. https://doi.org/10.1016/j.renene.2020.09.032

Yuan, Z., Liu, J., Zhang, Q., Liu, Y., Yuan, Y. and Li, Z. (2021), "Prediction and optimisation of fuel consumption for inland ships considering real-time status and environmental factors", *Ocean Eng.*, **221**, 108530. https://doi.org/10.1016/j.oceaneng.2020.108530

Zhang, Z., Ye, L., Qin, H., Liu, Y., Wang, C., Yu, X., Yin, X. and Li, J. (2019), "Wind speed prediction method using shared weight long short-term memory network and Gaussian process regression", *Appl. Energy*, **247**, 270-284. https://doi.org/10.1016/j.apenergy.2019.04.047

Zhang, X., Zhu, C., He, M., Dong, M., Zhang, G. and Zhang, F.

(2021), "Failure mechanism and long short-term memory neural network model for landslide risk prediction", *Remote Sens*., **14**(1), 166. https://doi.org/10.3390/rs14010166

Zhi, L., Li, Q.S., Fang, M. and Yi, J. (2017), "Identification of wind loads on supertall buildings using kalman filtering–based inverse method", *J. Struct. Eng*., **143**(4), 06016004. https://doi.org/10.1061/(ASCE)ST.1943-541X.0001691

Zhu, Q., Chen, J., Shi, D., Zhu, L., Bai, X., Duan, X. and Liu, Y. (2019), "Learning temporal and spatial correlations jointly: A unified framework for wind speed prediction", *IEEE Trans. Sustain. Energy*, **11**(1), 509-523. https://doi.org/10.1109/TSTE.2019.2897136